Surface & Coatings Technology 204 (2010) 3228–3233

Contents lists available at ScienceDirect

Surface & Coatings Technology

journal homepage: www.elsevier.com/locate/surfcoat

Residual stresses in titanium nitride thin films obtained with step variation of substrate bias voltage during deposition

A.G. Gómez [a,*], A.A.C. Recco [b], N.B. Lima [c], L.G. Martinez [c], A.P. Tschiptschin [b], R.M. Souza [a]

[a] Surface Phenomena Laboratory, Department of Mechanical Engineering, Polytechnic School of the University of São Paulo, Av. Professor Mello Moraes, 2231, São Paulo, Brazil
[b] Department of Metallurgy and Materials Engineering, Polytechnic School of the University of São Paulo, Av. Professor Mello Moraes, 2463, São Paulo, Brazil
[c] Nuclear and Energy Research Institute, IPEN, Av. Prof. Lineu Prestes, 2242, São Paulo, Brazil

ARTICLE INFO

Article history:
Received 28 July 2009
Accepted in revised form 10 March 2010
Available online 25 March 2010

Keywords:
Magnetron sputtering
Titanium nitride
X-ray diffraction
Stress gradients

ABSTRACT

In this work, a series of depositions of titanium nitride (TiN) films on M2 and D2 steel substrates were conducted in a Triode Magnetron Sputtering chamber. The temperature; gas flow and pressure were kept constant during each run. The substrate bias was either decreased or increased in a sequence of steps. Residual stress measurements were later conducted through the grazing X-ray diffraction method. Different incident angles were used in order to change the penetration depth and to obtain values of residual stress at different film depths. A model described by Dolle was adapted as an attempt to calculate the values of residual stress at each incident angle as a function of the value from each individual layer. Stress results indicated that the decrease in bias voltage during the deposition has produced compressive residual stress gradients through the film thickness. On the other hand, much less pronounced gradients were found in one of the films deposited with increasing bias voltage.

© 2010 Elsevier B.V. All rights reserved.

1. Introduction

The deposition of thin films on substrates is usually inherently associated with the development of residual stresses [1,2]. Mechanical equilibrium between substrate and film, combined with the fact that the film is thinner than the substrate, leads to higher stresses (in absolute values) in the film than in the substrate.

The level of film residual stresses depends on processing parameters [3–7] such as substrate temperature, substrate bias, operating pressure, coating thickness and deposition rate. In general, Physical Vapor Deposition (PVD) processes result in compressive stresses on the order of a few GPa, although compressive values above 10 GPa can be reached [8–11]. Such values may affect the behavior of the coated system in a given application. In particular, data in the literature [12–15] indicate that high compressive residual stresses can improve the wear resistance of these systems. However, higher compressive stresses also increase the possibility of film detachment during system use in tribological applications [12,13].

In theory, one could think that the imposition of a stress gradient in the film could be beneficial to improve the tribological behavior of coated systems. Along these lines, lower levels of compressive residual stresses at the film/substrate interface would decrease the tendency for film detachment and a gradual increase in compressive values towards the surface would improve wear resistance. This idea is valid even when one considers that film debonding is caused by the force on the interface, which is the integral of the stress over the thickness of the film. In this case, for given values of film thickness and maximum compressive stress, lower values of this integral would be present in a condition with stress gradient than in one with no gradient. The idea of gradient film stresses can be found in the works by Fischer and Oettel [16] and Uhlman and Klein [17]. However, one of the challenges associated with such idea is to verify if the deposition procedure was successful in imposing the stress gradient and also to determine the residual stress values in such gradients using a non-destructive technique.

In thin films, two techniques are commonly used to measure residual stresses: deflection techniques based on the measurement of the radius of curvature of the specimen before and after deposition and X-ray diffraction techniques. In general, deflection techniques allow only the calculation of the average stress in the film.

Several diffraction techniques have been proposed to study the problem of stress and strain gradients in single (one material) thin films. Several authors [18–22] have studied strain distribution through grazing incidence X-ray diffraction (GIXD) techniques, where the penetration depth was varied by changing the incident angle of the beam. In all these works, the measurements were conducted at angles near the critical angle for total external reflection [23].

* Corresponding author. Tel.: +52 572 321 8077.
E-mail addresses: agomez@usp.br, adrianagomez@javerianacali.edu.co (A.G. Gómez).

0257-8972/$ – see front matter © 2010 Elsevier B.V. All rights reserved.
doi:10.1016/j.surfcoat.2010.03.016

Predecki et al. [24] proposed two GIXD methods in asymmetric geometry to obtain stress profiles. Those methods were based on different wavelengths and on the fixing of the incident angle of the beam. Genzel [25] calculated stress gradients based on the scattering vector method. Brennan et al. [26] and Leung et al. [27] used a variation of the conventional $\sin^2\psi$ method to determine stress as a function of penetration depths. Marques et al. [28] and Peng et al. [29] studied residual stress gradients by means of pseudo-grazing incidence X-ray diffraction method (PGIXRD), which is based on the conventional $\sin^2\psi$ method in a 4-circle goniometer. In the method proposed by Kumar et al. [30], the penetration depth is modified by employing a combination of χ and ω tilting. Van Acker et al. [31] proposed the Low-Incident-Beam-Angle Diffraction (LIBAD) method to determine stress profiles of thin films by measuring the stresses at different incident beam angles. Rafaja, et al. [32] studied TiN coatings deposited by Chemical Vapor Deposition (CVD). These authors implanted metal ions of different species in order to produce residual stress gradients.

The methods mentioned above were employed to determine residual stresses in thin films produced with constant deposition parameters. Little work has been conducted in order to verify if the variation of the parameters selected during deposition results in stress gradients. One exception is the work by Wohlschologel et al. [33], who have studied the effect of temperature variation during deposition. Another exception is the work by Fischer and Oettel [16], who have studied residual stress gradients during the deposition of TiN films produced by reactive magnetron sputtering. These authors have analyzed the effect of substrate bias, as well as that of alternating and pulsed bias voltage. The residual stress gradients were measured using an asymmetric diffraction arrangement in Seemann-Bohling focusing, combined with stepwise removal of the film layers by mechanical polishing.

The objective of this work is twofold: Initially, similar to Fischer and Oettel [16], to verify the possibility of imposing stress gradients in thin films by changing the process parameters during deposition. Secondly, to adapt a model available in the literature [34] in order to evaluate these gradients using a non-destructive technique. The analysis was conducted on TiN films deposited with variations of substrate bias voltage in a Triode Magnetron Sputtering chamber. The residual stresses were determined with the grazing incidence X-ray diffraction method (GIXRD), and different angles of incidence were used in order to analyze stress gradients.

2. Experimental details

2.1. TiN deposition

TiN films were deposited on steel substrates. A hybrid duplex treatment was carried out in all cases, in a home built hybrid reactor, where pulsed plasma nitriding and triode unbalanced reactive magnetron sputtering are conducted in the same cycle [35]. Plasma nitriding was conducted in an atmosphere of N_2 (4 sccm), H_2 (80 sccm) and Ar (30 sccm), at a pressure of approximately 3×10^{-3} Torr, and temperature of 520 °C. Then, a titanium interlayer (with thickness ~100 nm) was deposited in order to have a better TiN adherence to the substrate [36]. Finally, the TiN films were deposited in an atmosphere of N_2 (4 sccm) and Ar (20 sccm) at a temperature of 300 °C and pressure of approximately 3.5×10^{-3} Torr.

Three types of specimens were produced in this work: (i) films deposited without variation of substrate bias voltage during deposition (specimens S1, S2, S3, S4 and S5), (ii) films deposited with increasing substrate bias voltage (specimens G1D2 and G3M2), and (iii) films deposited with decreasing substrate bias voltage (specimens G2D2 and G4M2). Details of the substrates and deposition conditions are shown in Table 1. In all cases, the total film thickness was measured by looking at the specimen cross-section in a Scanning Electron Microscope.

Table 1
Deposition conditions for TiN thin films.

Sample	Substrate material	Layer	Time (min)	Bias (V)	Film thickness (μm)
G1D2	AISI D2	1	45	−20	≈2.4
		2	45	−40	
		3	45	−100	
		4	45	−150	
		5	45	−200	
G2D2	AISI D2	1	45	−200	≈2.0
		2	45	−150	
		3	45	−100	
		4	45	−40	
		5	45	−20	
G3M2	AISI M2	1	45	−20	≈1.4
		2	45	−40	
		3	45	−80	
		4	45	−100	
G4M2	AISI M2	1	45	−100	≈1.4
		2	45	−80	
		3	45	−40	
		4	45	−20	
S1	AISI D2	1	120	−20	≈1.5
S2		1	120	−40	
S3		1	120	−100	
S4		1	120	−150	
S5		1	120	−200	

2.2. Residual stress measurements

In the GIXRD method the incident beam is kept constant at a low and constant incidence angle (α) and the position of the detector varies along the goniometer circle registering data at several (hkl) reflections.

The residual stress was calculated from the slope of the a^{hkl} vs. $f(\psi)$ plot [8], with $f(\psi) = ½S_2^{hkl} + 2S_1^{hhk} sin^2\psi$. The angle ψ is defined as $\psi = \theta - \alpha$, where θ and α are the Bragg angle and the angle of incidence, respectively. The a^{hkl} (lattice parameteres for each reflection) values were obtained by fitting the peak profiles by applying the Rietveld method using the GSAS + EXPGUI software [37,38].

S_1^{hkl} and $½S_2^{hkl}$, the X-ray elastic constants (XECs), were calculated for the different lattice planes (hkl) using Eq. (1) [39], in which S_2^m and S_1^m are the mechanical XECs calculated from the global value of the material Young's modulus (E^m) and Poisson's ratio (v^m), A_{XC} is the anisotropy factor and Γ^{hkl} is the crystallographic factor of each plane hkl, $\Gamma^{hkl} = (h^2k^2 + k^2l^2 + l^2h^2)/(h^2 + k^2 + l^2)^2$. The value of E^m used in this work (353 GPa) was based on the value obtained [35] for TiN films deposited using the same reactor as the one in the present work and v^m was taken as 0.25 [40]. In the absence of a value of A_{XC} calculated specifically for the film, or layers, obtained in this work, the procedure adopted by Atar et al. [41] was chosen, i.e. the value (0.733) calculated experimentally by Perry et al. [42] was selected.

$$\frac{1}{2}S_2^{hkl} = \frac{1}{2}S_2^m\left\{1 + \left[3.(\Gamma^m - \Gamma^{(hkl)}).\left(5\frac{(A_{XC}-1)}{(3 + 2A_{XC})}\right)\right]\right\}$$

$$S_1^{hkl} = S_1^m - \frac{1}{2}S_2^m\left\{(\Gamma^m - \Gamma^{(hkl)}).\left(5\frac{(A_{XC}-1)}{(3 + 2A_{XC})}\right)\right\} \quad (1)$$

For specimens produced with variation of bias, different angles of incidence were selected in order to measure the residual stresses at different beam penetration depths. The angles were chosen according to the number of layers and the film thickness.

Measurements on specimens G1D2 and G2D2 at the angles of incidence of 1.5°, 2.5°, 3.5° and 4.5°, were conducted at LNLS —

Brazilian Synchrotron Light Laboratory, using X-rays at the energy of 8.04 keV. Divergence slits were employed in the primary (aperture 0.5 mm) and in the diffracted beam (aperture 1.0 mm). A graphite analyzer was also used in this case. The diffraction planes scanned were (111), (200), (220), (311), (222), (331) and (420).

Measurements on specimens G1D2 and G2D2, at the incident angles of 6°, 8° and 10° were conducted in a Rigaku RINT Ultima+ diffractometer, in which parallel beam optics were used to reduce the divergence of the beam. Horizontal Soller slits were positioned during the analysis and a flat graphite monochromator was also used. The generator was operated at 40 kV and 30 mA using CuKα radiation. Automatic alignment of the specimen surface was conducted once a new specimen was placed on the holder. Diffraction planes (111), (200), (220), (222) and (420) were scanned at steps of 0.05° and different counting times were selected for each scan, in order to allow the same statistics for the different peak intensities (varying from 25 to 100 s).

Specimens G3M2 and G4M2 were entirely analyzed in the Rigaku Ultima+ diffractometer at incident angles of 1.5°, 3.5°, 6° and 8°, using the diffraction conditions described previously.

For specimens S1 to S5, the residual stresses were measured only at an angle of incidence of 1.5° using synchrotron radiation, with the diffraction conditions described previously.

2.3. Model for calculation of residual stress

In X-ray diffraction, the intensity of the incident beam is attenuated exponentially by the specimen due to the material absorption. Therefore, if the specimen stress changes with the distance from the surface, the measured value is affected not only by the variation of the stress but also by any change in the penetration depth. In this case, the obtained information is averaged over the entire penetration depth of the beam. According to Dolle [34], the mean value of residual stress over a depth x can be calculated by:

$$\sigma = \frac{\int_0^t \sigma(x)\cdot e^{-x/\tau}dx}{\int_0^t e^{-x/\tau}dx} \quad (2)$$

where $\sigma(x)$ is the depth profile of stress, t is the thickness of the film, and τ is the mean penetration depth [32]. Eq. (2) permits obtaining, or approximating, the depth profile of the residual stresses in the film [24,32], if $\sigma(x)$ is a continuous function. However, in the case of multilayered coating systems, Eq. (2) must be corrected to consider that $\sigma(x)$ is not continuous [43]. The same is valid for films deposited with step variation of bias voltage. In this case, assuming that the procedure has succeeded in producing a step distribution of residual stresses, a system composed of N_L layers will have a mean stress over a depth x, at a given angle of incidence (α_i), given by:

$$\sigma(\alpha_i) = \sum_{n=1}^{N_L} I_n(\alpha_i)\sigma_n \quad (3)$$

where σ_n is the mean residual stress of layer and n, $i=1,2,\ldots,N_\alpha$, is the number of the angle of incidence that is considered. Furthermore, N_α is the total number of angles of incidence measured in each sample, and

$$I_n(\alpha) = \frac{\int_{t_{n-1}}^{t_n} e^{-x/\tau}dx}{\int_o^t e^{-x/\tau}dx} \quad (4)$$

For example, for specimen G1D2, composed of five layers, the residual stress over a depth x at the angle of incidence of 8° can be calculated by:

$$\sigma(8°) = \frac{\int_0^{0.42} e^{-x/\tau}dx\cdot\sigma_1 + \int_{0.42}^{0.84} e^{-x/\tau}dx\cdot\sigma_2 + \int_{0.84}^{1.26} e^{-x/\tau}dx\cdot\sigma_3 + \int_{1.26}^{1.68} e^{-x/\tau}dx\cdot\sigma_4 + \int_{1.68}^{2.1} e^{-x/\tau}dx\cdot\sigma_5}{\int_0^{2.1} e^{-x/\tau}dx} \quad (5)$$

Note that in Eq. (4) the effect of the angle of incidence is considered through the value of τ.

Since the values of σ_n are unknown, the values of stress measured in the films deposited at constant bias voltage (S1 to S5) were used to calculate the mean stress at each angle of incidence.

In this work, Eq. (3) was also used in the opposite direction, i.e. in an attempt to calculate the residual stress value in each layer based on the average residual stresses obtained in a given specimen at each of the angles of incidence. In other words, this equation was used to find the values of σ_n that would best provide the N_α values of $\sigma(\alpha_i)$ obtained experimentally for a given specimen. For specimens G1D2 and G2D2, the stress over a depth was measured at seven angles of incidence, then seven equations were obtained (N_α is 7), and these specimens are composed of 5 layers (N_L is 5). Thus, a system of 7 equations and 5 variables was obtained for these two specimens. For specimens G3M2 and G4M2 N_α is 4 and N_L is 4, then for each one of these other two specimens a system of 4 equations and 4 variables was obtained. Each one of these systems of equations was solved by the least squares method using an optimization algorithm. Then, the problem can be formulated by the following optimization problem:

$$\min F = \sum_i \left[1 - \frac{1}{\sigma(\alpha_i)}\sum_n I_n(\alpha_i)\sigma_n\right]^2 \text{ where } i = 1,2,\ldots,N_\alpha \text{ and } n = 1,2,\ldots,N_L \quad (6)$$

σ_n

such that: $\sigma_{min} < \sigma_n < 0$.

F is the objective function and σ_n is the variable of the project. The values of σ_n were constrained at values between 0 and σ_{min}, where σ_{min} is −12 GPa. This range was defined since, in general, films deposited by PVD processes result in compressive stresses, and the experimental results obtained in this work never overcame −12 GPa.

The optimization problem was solved using a Matlab algorithm (solnp.m), which implements the sequential quadratic programming method (QP) in order to solve multi-variable optimization problems with constraints [44].

3. Results and discussion

Fig. 1 presents the residual stress values calculated for specimens S1 to S5, deposited with constant bias voltage. In this figure, the vertical error bars were calculated based on the fitting of the a^{hkl} vs. $f(\psi)$ plot by linear regression. As expected, the compressive residual stress level initially increased as the bias voltage increased. This behavior has been previously reported in several works regarding thin films deposited by sputtering [4,9,40]. Usually, the application of bias voltage to the substrate produces acceleration of ions towards the substrate, which collide against its surface at high speeds, resulting in high values of compressive stress during the film growth [6]. Some authors have found that the stresses reach a maximum value as the negative bias substrate increases [40,45], which, based on the results in Fig. 1, were observed in this work.

Fig. 2 shows a comparison between the experimental results of specimens deposited with variation of bias voltage, and the values of stress over a depth at each angle of incidence, calculated using the model in Eq. (3). In specimens G2D2 and G4M2, which were

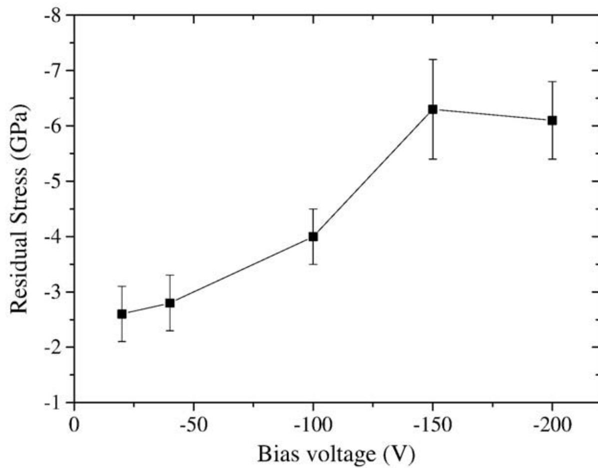

Fig. 1. Residual stresses of TiN films as a function of the substrate bias voltage during deposition.

deposited with decreasing bias voltage, Fig. 2 indicates smaller compressive residual stress levels near the surface and higher residual stresses closer to the film/substrate interface. This behavior was expected since lower stresses should be associated with lower bias. In terms of specimens G1D2 and G3M2, in which the bias voltage was increased during deposition, high compressive stresses were expected at the surface and smaller stresses were expected at the interface, as previously obtained by Fischer and Oettel [16], which found differences of approximately 3 GPa between the interface and the surface for TiN films deposited by reactive magnetron sputtering with increasing bias from 0 to −235 V. However, in specimen G1D2 the difference found in residual stress level between the surface and the interface was not significant. In specimen G3M2 a difference of 1 GPa was observed between the interface and the surface.

In general, Fig. 2 shows that the trend in residual stress values predicted by the model is in agreement with the experimental results, although some discrepancy can be observed in terms of the absolute values.

Among several possibilities that exist to explain the differences between the experimental and predicted results, this work will mention three: i) the model in Eq. (3) is invalid, ii) the deposition procedure was successful in imposing a step variation in film residual stresses, but the values in each layer are different from those of the films deposited with constant bias and iii) the procedure was not successful in imposing a step variation in film residual stresses, i.e. stress values change along film thickness, but stress variation is not sharp, or approximately sharp, when going from one layer to the next one.

In principle, the first option can be left aside, since the model in Eq. (3) was adapted from the model by Dolle and presents similarities with the approach by Klaus et al. [43].

The literature does not provide much information regarding options ii and iii. The few works correlating film residual stresses with the variation in the parameters selected during deposition were not detailed to the point of indicating, for example, how abrupt is the change in the stresses in going from one layer to the next one, and, more specifically, how accurate it would be to consider the stress variation as a sequence of well-defined steps. Thus, in terms of options ii and iii, the optimization method in Eq. (6) was applied, providing the results shown in Fig. 3. In this figure, the open squares represent the values of residual stress calculated for films deposited at constant bias voltage (Fig. 1). Note that the results obtained based on the optimization procedure do not have any clear restriction in terms of physical meaning, providing further evidence that the model by Dolle is applicable in this case.

In terms of the values that were obtained, the results of the optimization procedure presented in Fig. 3b) suggest that option "ii", above, has occurred for the specimens produced with decreasing bias. In this case, although differences exist in terms of the maximum residual stress value and the voltage at which the residual stresses reach the maximum, the trend was similar to that of the specimens deposited with constant bias voltage (Fig. 1). Interestingly, in Fig. 3b) the layer stresses to produce the values in Fig. 2 were almost identical for specimens with D2 and M2 substrates. On the other hand, the optimization procedure for specimens produced with increasing bias (Fig. 3a) did not provide similar results for both substrates. In this case, although the optimization values for specimen G3M2 suggest that the differences in experimental and predicted results were due to the layer stress values used in Eq. (3), the optimization results suggest that no stress gradient was obtained for specimen G1D2. At this point, no reason was found to explain why such differences may occur for the two films produced with increasing bias, especially when one considers that the differences were basically regarding the substrate and film thickness.

In addition to the three options cited in the previous paragraphs, it is worth mentioning that a uniform distribution of film residual stresses is difficultly obtained, even in the cases where the entire deposition is conducted with constant parameters [16,46,47]. Therefore, it would be possible to question the use of constant residual

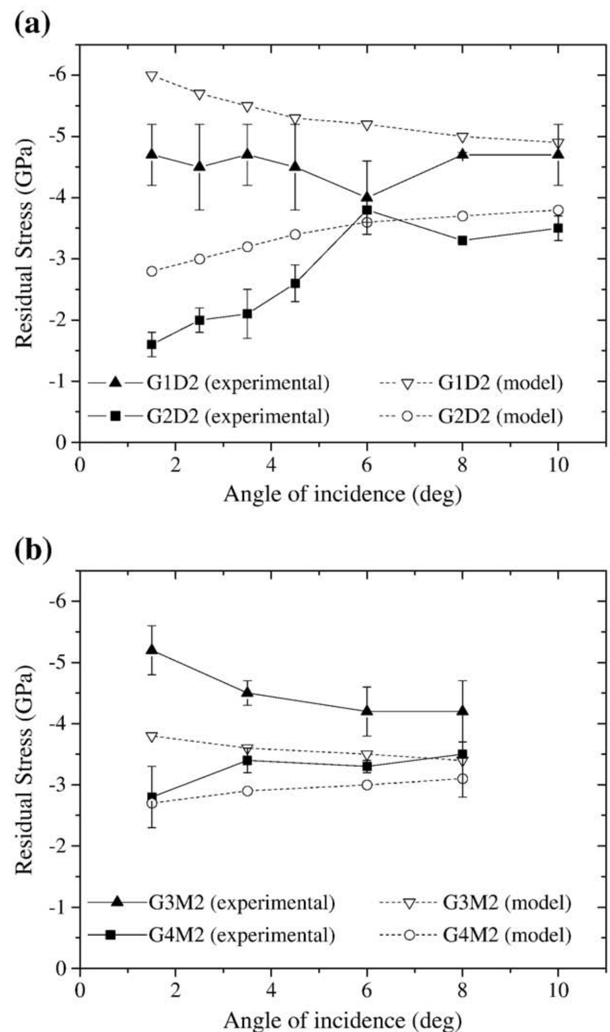

Fig. 2. Comparison between the experimental values of residual stress of specimens deposited with variation of bias voltage, and the results of stress over a depth calculated using the model of (a) specimens deposited on AISI D2 substrates, and (b) specimens deposited on AISI M2 substrates.

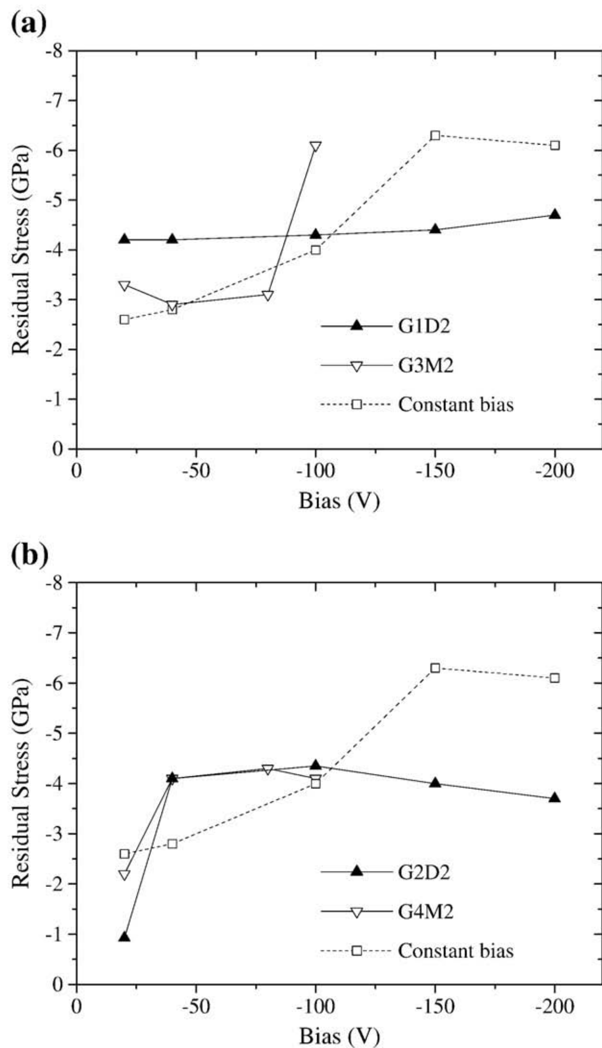

Fig. 3. Values of mean stress of each layer obtained using an optimization procedure for specimens deposited with a) increasing substrate bias voltage and b) decreasing substrate bias voltage.

stress values for each of the N_L layers in each specimen. However, it is important to observe that many works that present stress gradients with thickness for sputtered films deposited with constant conditions [46,47] indicate that stresses are more compressive close to the film/substrate interface, become less compressive when moving away from the interface and stabilize at an approximately constant value above a given thickness. In many cases, this thickness value is on the order of a few hundreds of nm. As previously explained, the intensity of incident X-ray beams are gradually attenuated by the specimen, such that most of the information in GIXRD is obtained from regions close to the surface, independent of the value of the fixed incident angle. Thus, if films deposited with constant parameters present thickness higher than 1 μm, it is possible to expect that the stress gradient close to the interface would not have a significant effect on the residual stress values measured at different incident fixed angles.

The decrease of compressive residual stresses with increasing thickness has been related to the coarsening of film columnar grains [16] and to the change of crystal orientation from <001> in early film growth stages to <111> in later stages of the deposition [47]. None of these possibilities may be definitely related to the formation of new stress gradients in films deposited with varying parameters, when moving from one layer to the next one. The same is valid considering that all layers are formed by TiN films. Thus, no clear reason exists to deduce that the stress gradient close to the film/substrate interface would significantly affect the measurements conducted on 1.5 μm-thick films prepared with step variation of bias during deposition. Once again, more detailed data on films deposited according to these conditions are still required for the confirmation of this statement.

4. Conclusions

A model described by Dolle was adapted to calculate the residual stresses as a function of beam penetration depth for the cases where deposition was conducted to impose a step variation in residual stresses along the film thickness. Since the real values in each layer are unknown, the values of stress measured in the films deposited at constant bias voltage were used in the calculations. The results were compared with the experimental ones, providing good qualitative agreement in all cases.

An optimization procedure was later conducted to analyze the individual layer values that, selecting the adapted model, would provide the best agreement with the experimental values calculated as a function of penetration depth. The results suggest that, in most cases, a step variation in residual stresses may have been obtained, and that the differences between experimental and predicted results are due to the stress value selected for each layer. On the other hand, the optimization procedure suggests that no step variation in residual stresses was obtained for one of the specimens produced with increasing bias.

Acknowledgements

This research was supported by LNLS — Brazilian Synchrotron Light Laboratory/MCT, under proposal D12A-XRD1 6680. The authors are grateful to the Laboratório de Cristalografia – Instituto de Física– Universidade de São Paulo and to CNPq (National Council of Technological and Scientific Development) for grants 303780/2008-8 and 150966/2009-1.

References

[1] F. Spaepen, Acta Mater. 48 (2000) 31.
[2] G.C.A.M. Jansen, Thin Solid Films 515 (2007) 6654.
[3] S. Ulrich, H. Holleck, J. Ye, H. Leiste, R. Loos, M. Stüber, P. Pesch, S. Sattel, Thin Solid Films 437 (1–2) (2003) 164.
[4] C.A. Carrasco, V. Vergara, R. Benavente, N. Mingolo, J.C. Rios, Mater. Charact. 48 (1) (2002) 81.
[5] Y. Pauleau, Vacuum 61 (2–4) (2001) 175.
[6] O. Knotek, R. Elsing, G. Krämer, F. Jungblut, Surf. Coat. Technol. 46 (3) (1991) 265.
[7] R. Machunze, G.C.A.M. Janssen, Surf. Coat. Technol. 203 (1–2) (2008) 550.
[8] A.J. Perry, Thin Solid Films 214 (2) (1992) 169.
[9] C. Quaeyhaegens, G. Knuyt, L.M. Stals, J. Vac. Sci. Technol. A 14 (4) (1996) 2462.
[10] M. Benegra, D.G. Lamas, M.E. Fernandez de Rapp, N. Mingolo, A.O. Kunrath, R.M. Souza, Thin Solid Films 494 (1–2) (2006) 146.
[11] K. Holmberg, H. Ronkainen, A. Laukkanen, K. Wallin, S. Hogmark, S. Jacobson, U. Wiklund, R.M. Souza, P. Ståhle, Wear 267 (2009) 2142.
[12] S. Bull, Wear 233–235 (1999) 412.
[13] R.C. Cozza, D.K. Tanaka, R.M. Souza, Surf. Coat. Technol. 201 (7) (2006) 4242.
[14] J. Gunnars, A. Alahelisten, Surf. Coat. Technol. 80 (3) (1996) 303.
[15] T.Z. Kattamis, M. Chen, S. Skolianos, B.V. Chambers, Surf. Coat. Technol. 70 (1) (1994) 43 (K).
[16] K. Fischer, H. Oettel, Surf. Coat. Technol. 97 (1–3) (1997) 308.
[17] E. Uhlmann, K. Klein, Surf, Coat. Technol. 131 (1–3) (2000) 448.
[18] M. Van Leeuwen, J.D. Kamminga, E.J. Mittemeijer, J. Appl. Phys. 86 (1999) 1904.
[19] M.F. Doerner, S. Brennan, J. Appl. Phys. 63 (1) (1988) 126.
[20] C.J. Shute, J.B. Cohen, J. Appl. Phys. 70 (4) (1991) 2104.
[21] R. Venkatraman, P.R. Besser, J.C. Bravman, S. Brennan, J. Mater. Res. 9 (2) (1994) 328.
[22] S.G. Malhotra, Z.U. Rek, S.M. Yalisobe, J.C. Billelo, J. Appl. Phys. 79 (9) (1996) 6872.
[23] W.C. Marra, P. Eisenberger, A.Y. Cho, J. Appl. Phys. 50 (11) (1979) 6927.
[24] P. Predecki, X. Zhu, B. Ballard, Adv. X-Ray Anal. 36 (1993) 237.
[25] C.H. Genzel, Phys. Stat. Solidi A 156 (2) (1996) 353.
[26] S. Brennan, W.D. Nix, Phys. B 283 (1–3) (2000) 125.
[27] O.S. Leung, A. Munkholm, S. Brennan, W.D. Nix, J. Appl. Phys. 88 (3) (2000) 1389.
[28] M.J. Marques, A.M. Dias, P. Gergaud, J.L. Lebrun, Mater. Sci. Eng. A 287 (1) (2000) 78.
[29] J. Peng, V. Ji, W. Seiler, A. Tomescu, A. Levesque, A. Bouteville, Surf. Coat. Technol. 200 (8) (2006) 2738.

[30] A. Kumar, U. Welzel, E.J. Mittemeijer, J. Appl. Crystallogr. 39 (5) (2006) 633.
[31] K. Van Acker, L. De Buyser, J.P. Celis, P. Van Houtte, J. Appl. Crystallogr. 27 (1) (1994) 56.
[32] D. Rafaja, V. Valvoda, A.J. Perry, J.R. Treglio, Surf. Coat. Technol. 92 (1–2) (1997) 135.
[33] M. Wohlschlogel, W. Baumann, U. Welzel, E.J. Mittemeijer, Mater. Sci. Forum 524–525 (2006) 19.
[34] H. Dolle, J. Appl. Cryst. 12 (6) (1979) 489.
[35] A.A.C. Recco, I.C. Oliveira, M. Massi, H.S. Maciel, A.P. Tschiptschin, Surf. Coat. Technol 202 (4–7) (2007) 1078.
[36] K.A. Pischow, L. Eriksson, E. Harju, A.S. Korhonen, E.O. Ristolainen, Surf. Coat. Technol. 58 (3) (1993) 163.
[37] A.C. Larson, R.B. Von Dreele, General Structure Analysis System (GSAS), Los Alamos National Laboratory Report LAUR 86-748, 1994.
[38] B.H. Toby, J. Appl. Crystallogr. 34 (2) (2001) 210.
[39] R.Y. Fillit, A.J. Perry, Surf. Coat. Technol. 36 (3–4) (1988) 647.
[40] R.F. Bunshah (Ed.), Handbook of Hard Coatings: deposition technologies, properties and applications, Noyens Publications, New Jersey, 2001, pp. 108–180.
[41] E. Atar, C. Sariouglu, H. Cimenoglu, E.S. Kayali, Surf. Coat. Technol. 191 (2–3) (2005) 188.
[42] A.J. Perry, Thin Solid Films 193/194 (1) (1990) 463.
[43] M. Klaus, Ch. Genzel, H. Holzschuh, Thin Solid Films 517 (2008) 1172.
[44] Y. Ye. Interior algorithms for linear, quadratic, and linearly constrained non-linear programming. Ph. D. Thesis, Department of EES, Stanford University (Stanford, CA), 1987.
[45] C.A. Davis, Thin Solid Films. 226 (1) (1993) 30.
[46] H. Köstenbauer, G.A. Fontalvo, M. Kaap, J. Keckes, C. Mitterer, Surf. Coat. Technol. 201 (8) (2007) 4777.
[47] R. Machunze, G.C.A.M. Janssen, Thin Solid Films 517 (20) (2009) 5888.